

Interstellar H_3^+

Takeshi Oka[†]

Departments of Chemistry and Astronomy and Astrophysics, Enrico Fermi Institute, University of Chicago, Chicago, IL 60637

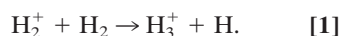
Edited by William Klemperer, Harvard University, Cambridge, MA, and approved June 13, 2006 (received for review February 4, 2006)

Protonated molecular hydrogen, H_3^+ , is the simplest polyatomic molecule. It is the most abundantly produced interstellar molecule, next only to H_2 , although its steady state concentration is low because of its extremely high chemical reactivity. H_3^+ is a strong acid (proton donor) and initiates chains of ion-molecule reactions in interstellar space thus leading to formation of complex molecules. Here, I summarize the understandings on this fundamental species in interstellar space obtained from our infrared observations since its discovery in 1996 and discuss the recent observations and analyses of H_3^+ in the Central Molecular Zone near the Galactic center that led to a revelation of a vast amount of warm and diffuse gas existing in the region.

Although it took many years to detect the first signal of interstellar H_3^+ , subsequent observations have revealed the ubiquity of this molecular ion that plays the pivotal role in interstellar chemistry. It has now been well established that H_3^+ exists abundantly not only in dense molecular clouds as predicted by chemical model calculations but also in diffuse clouds, and that the total amount of H_3^+ in a diffuse cloud is orders of magnitude higher than in a dense cloud. The surprise continued, culminating in the recent discovery of H_3^+ in the $(J, K) = (3, 3)$ metastable rotational level that is 361 K above the ground level and the resultant revelation of a vast amount of gas with high temperature and low density in the Central Molecular Zone (CMZ) of the Galactic center. Here, I trace this inspiring development from a unified perspective of molecular astrophysics and project into the future.

H_3^+ , the Initiator of Interstellar Chemistry

Within a decade and a half of the discovery of H_3^+ by J. J. Thomson in 1911 (1), it was clear that H_3^+ was the most abundant ion in ordinary hydrogen discharges. Hogness and Lunn (2) inferred that H_3^+ was produced by a secondary process, the ionization of H_2 into H_2^+ by electron impact followed by the ion-neutral reaction,



It was later shown that this reaction is extremely efficient with a high exothermicity of 1.7 eV and a large Langevin rate constant of $k_L = 2 \times 10^{-9} \text{ cm}^3 \text{ s}^{-1}$. By 1961, the efficiency of this reaction and the dominance of H_3^+ in hydrogen plasmas were so well established that McDaniel and colleagues (3) advocated the possibility of detecting interstellar H_3^+ “because this molecular ion may be present under some circumstances to the virtual exclusion of H_2^+ .”

In 1973, after the avalanche of radio astronomical discoveries of interstellar molecules triggered by Townes and colleagues, Watson (4) and Herbst and Klemperer (5) showed that H_3^+ is not only

the most abundantly produced molecular ion in interstellar space via cosmic ray ionization but also plays a crucial role in interstellar chemistry. Because the proton affinity of H_2 (4.4 eV) is lower than that of almost all atoms and molecules (with the notable exception of He, N, and O_2), H_3^+ acts as a universal proton donor (acid) through the proton hop reaction,



which also has a large Langevin rate constant k_X . Once protonated, HX^+ is far more active than the neutral X and leads to a chain of ion-neutral reactions. For example, a protonated oxygen atom, HO^+ , produces a hydronium ion after a series of hydrogen abstraction reactions with H_2 , $\text{HO}^+ \rightarrow \text{H}_2\text{O}^+ \rightarrow \text{H}_3\text{O}^+$, which recombines with an electron to form interstellar water. Without the protonation of atoms and molecules by H_3^+ , the formation of interstellar molecules would proceed much more slowly. Because timely production of a large amount of molecules is essential for cooling gravitationally condensing gas, H_3^+ plays a crucial role in star formation.

Simple Chemistry and Unique Astrophysical Probe

Because 99.9% of atoms in the Universe are hydrogen (92.1%) and helium (7.8%), interstellar chemistry is a hydrogen-dominated chemistry. Initially, interstellar gas was thought to be atomic, but it has become increasingly clear that molecular hydrogen is the most abundant species in the interstellar medium. This is true not only in dense molecular clouds with densities of 10^4 cm^{-3} or higher that are gravitationally bound and on their way to star formation, but also in diffuse clouds with densities of $\approx 10^2 \text{ cm}^{-3}$. In the Galaxy, those clouds together contain perhaps $\approx 80\%$ of interstellar matter whose total mass is on the order of $\approx 3\%$ of the total mass of the stars (6). This vast amount of H_2 is continuously ionized by the ubiquitous cosmic rays to produce H_2^+ . Because the reaction rate of Eq. 1, $k_L n(\text{H}_2)$, is higher than the ionization rate $\zeta \sim 3 \times$

10^{-17} s^{-1} by many orders of magnitude, the production rate of H_3^+ per unit volume is given by $\zeta n(\text{H}_2)$ both for dense and diffuse clouds.

The destruction mechanism for H_3^+ , however, differs in dense and diffuse clouds. In dense clouds where carbon atoms are mostly in CO, H_3^+ is mainly destroyed by reaction in Eq. 2 with $\text{X} = \text{CO}$ (we ignore O for simplicity), whereas in diffuse clouds where C is mostly atomic, H_3^+ is destroyed by recombination with electrons released from the photoionization of C. Equating the production rate $\zeta n(\text{H}_2)$ and the destruction rate $k_{\text{CO}} n(\text{H}_3^+) n(\text{CO})$ and $k_e n(\text{H}_3^+) n(e^-)$ for dense and diffuse clouds, respectively, we obtain the H_3^+ number densities

$$n(\text{H}_3^+)_{\text{dense}} \approx (\zeta/k_{\text{CO}})[n(\text{H}_2)/n(\text{CO})] \quad [3]$$

and

$$n(\text{H}_3^+)_{\text{diffuse}} \approx (\zeta/k_e)[n(\text{H}_2)/n(e^-)]. \quad [4]$$

If we assume the same ζ for dense and diffuse clouds, and $[n(\text{H}_2)/n(\text{CO})] \sim [n(\text{H}_2)/n(e^-)]$, $n(\text{H}_3^+)_{\text{diffuse}}$ is calculated to be 100 times lower than $n(\text{H}_3^+)_{\text{dense}}$ because k_{CO} (due to the r^{-4} Langevin potential) is 100 times smaller than k_e (due to the long-range r^{-1} Coulomb potential).

A remarkable aspect of Eqs. 3 and 4 is that $N(\text{H}_3^+)$ does not scale with cloud density [$\sim n(\text{H}_2)$] but is proportional to the ratios of $n(\text{H}_2)/n(\text{CO})$ and $n(\text{H}_2)/n(e^-) \sim n(\text{H}_2)/n(\text{C}^+)$, which are approximately constant for typical dense and diffuse clouds, respectively. This situation is shown schematically in Fig. 1. This special characteristic of H_3^+ , stemming from the fact that its production rate is linear to concentration rather than quadratic, makes H_3^+ a unique astrophysical probe. We can use it as a yardstick to measure the dimensions of clouds, because ob-

Conflict of interest statement: No conflicts declared.

This paper was submitted directly (Track II) to the PNAS office.

[†]E-mail: t-oka@uchicago.edu.

© 2006 by The National Academy of Sciences of the USA

and other groups. In the meantime the first nonterrestrial H_3^+ spectrum was observed in 1987 as strong emission from Jupiter, and emissions from Uranus and Saturn followed. The exciting development of H_3^+ spectroscopy in planetary ionospheres is outside the scope of this article, and readers are referred to reviews (16, 17). In the early 1990s, the first large two-dimensional infrared array detectors were installed in spectrometers, and this greatly enhanced the sensitivity and reliability of infrared spectroscopy, setting the stage for the next development.

Interstellar H_3^+ was detected on April 29, 1996 at the United Kingdom Infrared Telescope (UKIRT) toward the infrared stars AFGL 2136 and W33A, two bright young stellar objects that are deeply embedded in the natal dense clouds. After confirming on July 15 that the doublet Doppler shifts by an expected amount due to the motion of the earth, a paper was submitted. The extremely weak $R(1, 1)^-R(1, 0)$ doublet is shown in Fig. 2 (18). Their observed equivalent widths (integrated absorption) gave H_3^+ column densities of $4 \times 10^{14} \text{ cm}^{-2}$ and $6 \times 10^{14} \text{ cm}^{-2}$ for AFGL 2136 and W33A, respectively, corresponding to $\zeta L \sim 260 \text{ cm s}^{-1}$ and 380 cm s^{-1} . If we use the canonical ζ value of $\approx 3 \times 10^{-17} \text{ s}^{-1}$ (see, for example, refs. 19 and 20), we obtain pathlengths L of 3 pc and 4 pc for the clouds that are reasonable orders of magnitude. The temperatures of the clouds were determined from the intensity ratios of the doublet to be $\approx 35 \text{ K}$, which was also reasonable. For over two decades since 1973, the presence of H_3^+ had been assumed. Now, this species was finally observed with the amount predicted by model calculations. A big sigh of relief was heard from the community of interstellar chemistry (21, 22).

Although it took 15 years to detect the first signal of interstellar H_3^+ , once discovered, it seemed to be observable everywhere as long as a dense cloud had sufficiently long pathlength (23). By now, H_3^+ has been observed in more than a dozen dense clouds, and the measured values of ζL are $70\text{--}330 \text{ cm s}^{-1}$, just about the right order of magnitude for canonical values of the cosmic-ray ionization rate ζ and pathlength L . The temperatures of clouds $24\text{--}50 \text{ K}$ are also reasonable. For now, the H_3^+ chemistry in dense clouds is a happy story. Clouds with very high densities ($n \geq 10^6 \text{ cm}^{-3}$) and low temperatures ($T \sim 10 \text{ K}$), however, are a different story. In such clouds, most molecules other than H_2 and its isotopomers may be frozen onto grain, and the slightly exothermic reaction with HD may become the main destruction process, leading to extremely high deuterium fractionation. This interesting subject, developed in the

last few years, is outside the scope of this paper, and readers are referred to refs. 24 and 25.

Enigma of H_3^+ in Diffuse Clouds

If an observation confirms a prediction, it is gratifying but not really exciting. Luckily, it did not take too long before our observations revealed something unexpected. On July 11, 1997, during our survey of dense clouds (23), we detected very strong H_3^+ lines toward two infrared sources GC IRS 3 and GCS 3-2 near the Galactic center (26). Because the visual extinction $A_V \sim 30$ mag toward the Galactic center is caused more by diffuse clouds than dense clouds, this suggested the previously unforeseen possibility that H_3^+ may exist abundantly also in diffuse clouds.

Indeed, our observation later that night revealed a high column density of H_3^+ toward Cygnus OB2 No. 12, the archetypical sightline obscured by diffuse clouds. This faint red star discovered by Morgan and colleagues in 1954 is arguably the most intrinsically luminous star in the Galaxy, and its visual extinction of $A_V = 10.3$ is the highest known among optical stars (27). Nevertheless, its visual extinction is only $\approx 1/10$ that toward dense cloud sources like AFGL 2136 and W33A ($A_V \sim 100$), indicating, if we assume the same dust-to-gas ratio, that a 10-times-smaller amount of gas occupies a 10-times-longer path in the diffuse cloud than in the dense clouds. The H_3^+ number densities given in Eqs. 3 and 4 therefore predict that the H_3^+ column density in the diffuse clouds is $1/10$ of the dense clouds, which would have been hard to detect. Contrary to the expectation, we observed $N(\text{H}_3^+) = 3.8 \times 10^{14} \text{ cm}^{-2}$ (26, 28), which is comparable to the value toward AFGL 2136 and W33A. From Eq. 6, we obtain $\zeta L \sim 3 \times 10^4 \text{ cm s}^{-1}$ (even for $f = 1$), 100 times higher than that of dense clouds. The canonical value of $\zeta = 3 \times 10^{-17} \text{ s}^{-1}$ gives an extremely long path length of ≈ 300 pc, which occupies a sizable fraction of the distance to the star (1.7 kpc)! Such a huge cloud is unknown. Moreover, the density of the cloud, if distributed over such a long distance, would be $\approx 10 \text{ cm}^{-3}$ from the standard dust to gas ratio (29), hardly an environment to contain a large fraction of H_2 and thus H_3^+ . It is more likely from the observed value of $A_V \sim 10.3$ that L is on the order of 30 pc and that ζ is 10 times higher than the canonical value. This applies to all diffuse clouds as discussed later. Before jumping to this conclusion, however, we needed to examine the assumptions made for calculating ζL in Eq. 6.

The first suspect was the recombination rate constant k_e . Through the years, the laboratory measurements of this value

have been notoriously contradictory. A wide range of values spanning over four orders of magnitude had been reported by different experimental techniques (see ref. 30 for a review). Also, modern theoretical calculations had always given orders of magnitude lower value than the one used above. Such a low value of k_e would immediately explain the large observed H_3^+ column density in diffuse clouds. However, the experiments by Larsson and colleagues (30) using the ion storage ring have consistently given a higher value, on the order of $10^{-7} \text{ cm}^3 \text{ s}^{-1}$, since 1993. Finally in 2003, Kokouline and Greene (31, 64) presented an extensive theoretical calculation including the Jahn-Teller effect and gave a value of k_e that agrees with the experiment (9, 30). For now the experimental value of $k_e = 2.6 \times 10^{-7} \text{ cm}^3 \text{ s}^{-1}$ at 23 K (9) used above for Eq. 6 seems the most reliable one. However, because this rate constant is of overwhelming importance, more theoretical and experimental studies are desirable.

The second suspect was the possibility that the ratio $n(\text{H}_2)/n(e^-)$ is higher than the value used above due to an incomplete ionization of carbon atom. This was negated when we detected H_3^+ with a column density of $8 \times 10^{13} \text{ cm}^{-2}$ toward the prototypical optical star ζ Per (9). This bright star ($V = 2.86$) with low visual extinction ($A_V = 0.9$) is sufficiently unattenuated in the UV to allow observation of the forbidden spectrum of C^+ at $2,325.4 \text{ \AA}$. The observation showed that indeed the carbon atoms are mostly ionized.

Those results suggest strongly that ζ in diffuse clouds is indeed 10 times higher than in dense clouds. This is reasonable because the soft components of the cosmic ray are attenuated by high-density gas (32). The high value of $\zeta \sim 3 \times 10^{-16} \text{ s}^{-1}$ is beyond the limit set from observed abundances of HD and OH (33, 34), but a recent paper by Liszt (35) has shown that higher values of ζ are favored if neutralization of atomic ions on dust grains is properly taken into account. Liszt warns, however, that larger values of ζ do not simply increase the H_3^+ number density because the higher cosmic ray ionization will introduce ionization of H in addition to that of C.

Overall, the high column density of H_3^+ in the diffuse interstellar medium is a major enigma, along with the large abundance of CH^+ , which is yet to be understood.

The Ubiquitous H_3^+

Although not completely understood, the large column densities of H_3^+ in diffuse clouds have been well established observationally (36). Cygnus OB2 No. 12 [$V = 11.4$, $E(B - V) = 3.35$] and No.

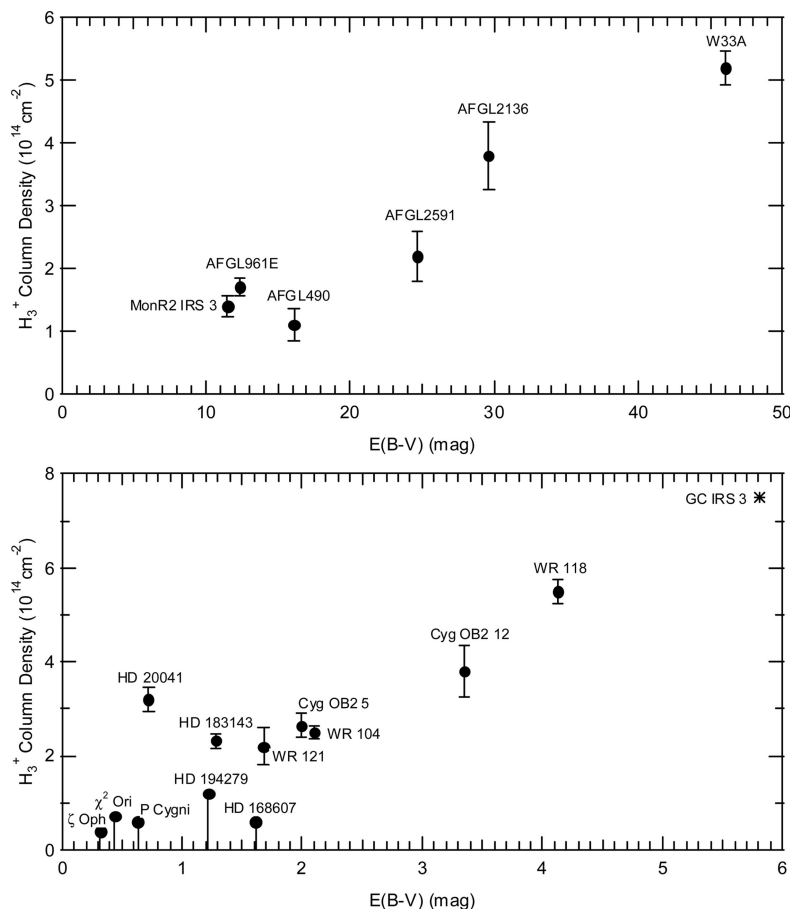


Fig. 3. Observed H_3^+ column densities versus color excess $E(B - V)$ for dense clouds (*Upper*) and diffuse clouds (*Lower*). Note that the two categories of clouds have comparable $N(H_3^+)$, although $E(B - V)$, and hence the amount of gas in the sightline, is 10 times lower for diffuse clouds than from dense clouds. (Reproduced from refs. 23 and 36.)

5 (9.2, 1.99), Wolf-Rayet stars WR 118 (22.0, 4.13), WR 104 (13.5, 2.10), WR 121 (11.9, 1.68), the prototypical diffuse interstellar bands sightline HD18 3143 (6.9, 1.28), HD 20041 (5.8, 0.70), and ζ Per (2.9, 0.31) all showed clear signals of H_3^+ , where $E(B - V)$ is the color excess that is $\approx 1/3$ of A_V . H_3^+ is ubiquitous; it exists in diffuse clouds as well as in dense clouds.

The observed H_3^+ column densities in dense and diffuse clouds versus their color excess are shown in Fig. 3. It is seen that $N(H_3^+)$ is approximately proportional to $E(B - V)$ (and thus to A_V), indicating that the cloud dimension is approximately proportional to A_V ; that is, the variations of A_V for these samples of clouds are due to variations of pathlength rather than density. From a least squares fitting of the observed values given in Fig. 3, we have

$$N(H_3^+)_{\text{dense}} \approx 3.6 \times 10^{12} \text{ cm}^{-2} A_V \quad [7]$$

and

$$N(H_3^+)_{\text{diffuse}} \approx 4.4 \times 10^{13} \text{ cm}^{-2} A_V, \quad [8]$$

i.e., the fractional abundance of H_3^+ in the gas is an order of magnitude higher in diffuse clouds than in dense clouds. Our attempt to find “translucent clouds” that may have $N(H_3^+)$ intermediate between dense and diffuse clouds is so far negative. Sightlines with relatively high A_V such as the Wolf-Rayet stars ($A_V = 13\text{--}5$) and the Stephenson objects ($A_V = 16\text{--}12$) all gave values on the straight line of diffuse clouds, suggesting that those so-called “translucent sightlines” are simply pileups of diffuse clouds and are not due to “translucent clouds.”

The total amount of H_3^+ in a diffuse cloud should be 100 times more than in a dense cloud because the pathlength through a diffuse cloud is 10 times higher than that through a dense cloud. The relative number of dense and diffuse clouds is not known, but it is very likely that the total amount of H_3^+ in dense clouds is much less than that in diffuse clouds!

Ideal Level Structure and Metastable H_3^+

The spectra so far discussed were mostly obtained by using the 3.6-m UKIRT on

Mauna Kea but also partly by using the 4-m Mayall Telescope on Kitt Peak. The absorption spectra were all starting from the lowest two rotational levels, $(J, K) = (1, 1)$ and $(1, 0)$. The advent of 8-m-class telescopes equipped with high-resolution spectrometers around the turn of the century has led us to the next major development. Before going into this, however, I need to discuss the rotational-level structure of H_3^+ in the ground vibrational state.

Fig. 4 shows rotational levels of H_3^+ labeled by the rotational quantum number J and its projection to the symmetry axis K . Because the proton is a fermion with spin $1/2$, the totally symmetric levels $(0, 0)$, $(2, 0)$, etc. are forbidden (broken lines) and levels with $K = 3n$ are occupied by *ortho*- H_3^+ ($I = 3/2$; red lines) and $K = 3n \pm 1$ by *para*- H_3^+ ($I = 1/2$; blue lines). The \pm signs beside levels show parity of the state, $(-1)^K$. Readers are referred to ref. 37 for more details.

Because H_3^+ is an equilateral triangle, there is no permanent dipole moment and hence no ordinary rotational spectrum. However, as initially considered for NH_3 (38), a breakdown of the geometrical symmetry due to centrifugal distortion may cause a small dipole moment and hence spontaneous emissions. Such emissions, that are slow and almost academic for NH_3 , are much faster for H_3^+ because of its smaller mass (39) and are competitive with collisions. For example, *para*- H_3^+ in the $(2, 2)$ level decays to the $(1, 1)$ ground level with a life time of 27 days, which corresponds to a critical density (at which collision rates become comparable to the spontaneous emission rate) of $\approx 200 \text{ cm}^{-3}$, just about the number density of diffuse clouds! On the other hand, *ortho*- H_3^+ in the $(3, 3)$ level cannot decay because the *ortho* \rightarrow *para* transition is forbidden and the $(2, 0)$ level is missing. H_3^+ in the $(3, 3)$ level is metastable and decays to lower levels only through collisions. Thus, in a low-density cloud of sufficiently high tem-

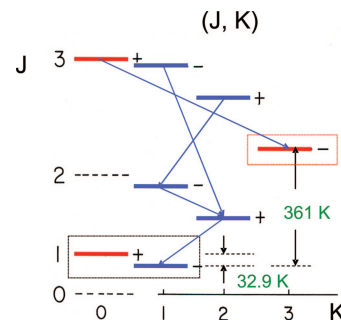


Fig. 4. Rotational levels of H_3^+ in the ground vibrational state. In the CMZ so far observed, most H_3^+ are populated in three levels: the $(1, 1)$ ground level (*para*- H_3^+), the $(1, 0)$ *ortho*-ground level, and the $(3, 3)$ *ortho*-metastable level. Blue arrows indicate spontaneous emissions. See ref. 41 for more detail.

perature, a very nonthermal distribution results between the metastable (3, 3) level and the unstable (2, 2) level.

H_3^+ in other higher rotational levels in Fig. 4 are all unstable and decay quickly to lower levels; the life times of the (3, 0), (3, 1), (3, 2), and (2, 1) levels are 3.8 h, 7.9 h, 16 h, and 20 days, respectively (39, 40). Thus, these levels are not populated unless the gas has both high temperature and high density, which we have not found so far for H_3^+ . For a low-temperature cloud, only the lowest two levels are populated. The (1, 0) ortho level is 32.9 K above the (1, 1) para level, approximately the temperature of the clouds (23, 36). The ratio of spin statistical weight $(2I + 1)$, 4:2, is approximately compensated by the Boltzmann factor and the spectral strength to make the intensities of the $R(1, 1)^u$ and $R(1, 0)$ lines in Figs. 3 comparable.

On the other hand, the (3, 3) metastable level is 361 K above the (1, 1) ground level, and its population is a sure sign of high temperature. The observed population ratio $n(3, 3)/n(1, 1)$ serves as a thermometer. Meanwhile, the observed ratio $n(3, 3)/n(2, 2)$ serves as a densitometer because the population of the (2, 2) unstable level is a sensitive function of cloud density. The four rotational levels, the (1, 1) ground level, the (1, 0) ortho ground level, the (2, 2) unstable level, and the (3, 3) metastable level, form an ideal level system for observing both cold and warm clouds. I cannot think of a better arrangement than this provided by nature!

Thermalization of H_3^+ and the resultant steady-state rotational distribution depends on a subtle interplay between radiative and collisional interactions. Although selection rules for spontaneous emission are rigorous and the aforementioned lifetimes are very accurate (perhaps to within 5%) (40), our knowledge of state-to-state collision-induced transitions is very limited. The simple level structure, however, allows us to calculate thermalization with some accuracy based on rough assumptions. We have used a simplifying assumption that collision-induced transitions occur completely randomly without selection rules (41). Such an assumption, used for strong collisions by van Vleck and Weisskopf in the early days of microwave spectroscopy (42), ignores the subsequently established nearly rigorous ortho \leftrightarrow para rule and the approximate selection rules for other quantum numbers governing collision-induced transitions (43). This is justified to a large extent for collisions between H_3^+ and H_2 because, unlike for neutral molecules,



is actually a chemical reaction and protons scramble in the activated complex $(H_5^+)^*$. Thus, unlike for neutral molecules, H_2 , H_2O , and NH_3 , collision-induced transitions from ortho to para level of H_3^+ are allowed as shown by laboratory experiments (44). We have used transition probabilities based only on the principle of detailed balancing and calculated $n(3, 3)/n(1, 1)$ and $n(3, 3)/n(2, 2)$ as a function of temperature and density of clouds. Readers are referred to ref. 41 for more details.

Discovery of Metastable H_3^+ in the Central Molecular Zone

The CMZ, a region of radius ≈ 200 pc of the Galactic center containing a large mass ($\approx 5 \times 10^7 M_\odot$) of dominantly molecular gas (45), is the treasure house of H_3^+ . The H_3^+ column density toward the CMZ is an order of magnitude higher than in other sightlines in the Galactic disk (46). Because the visual extinction toward the CMZ of $A_V \sim 30$ mag is caused more by diffuse clouds than by dense clouds, a large $N(H_3^+)$ is expected from Eq. 8, but the observed H_3^+ column density toward the Galactic center is higher by another factor of $\approx 5!$

Interstellar H_3^+ in the metastable (3, 3) level was discovered in this environment by using the 8.2-m Subaru Telescope (47). The discovery was facilitated by the wide wavelength coverage of its IRCS spectrometer equipped with an echelle and a

cross-dispersion grating that allows high-resolution spectroscopy ($R \sim 20,000$) without sacrificing wavelength coverage. The observed $R(3, 3)^u$ and $R(1, 1)^u$ lines are shown overlapped on the same velocity scale together with spectral lines of the CO 2-0 overtone band in Fig. 5. These spectra were observed toward GCS 3-2, a young star in the Quintuplet cluster (48) and the brightest infrared source ($L = 2.7$) in the CMZ.

The sharp peaks in the $R(1, 1)^u$ and CO spectra [but *not* in the $R(3, 3)^u$ spectrum] are absorptions by molecules in relatively cold and dense regions largely in the intervening spiral arms. Gas in the CMZ produces the $R(3, 3)^u$ spectrum and the “trough” of the $R(1, 1)^u$ spectrum that are nearly identical. These two featureless spectra with high-velocity dispersion ranging from -160 km s^{-1} to $+30 \text{ km s}^{-1}$ demonstrate the energetic, turbulent nature of the gas in the CMZ. Their nearly equal intensities, corresponding to a (3, 3)/(1, 1) excitation temperature of ≈ 200 K, demonstrate a high kinetic temperature. Further analyses based on more spectra taken under higher resolution at the 8-m Gemini South Telescope on Cerro Pachon, Chile, and UKIRT and a detailed model calculation (41) have led to a revelation of a new category of clouds.

Warm and Diffuse Clouds in the CMZ

It had been known mainly from radio-astronomical observations that the CMZ

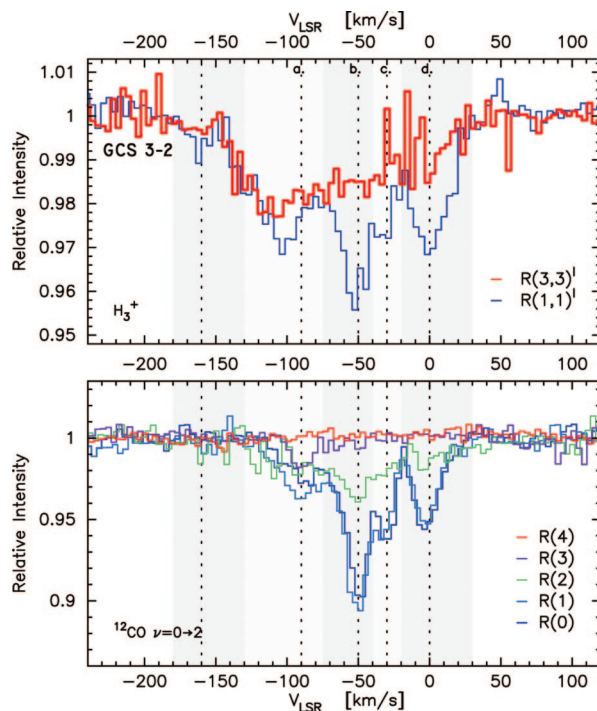


Fig. 5. Spectra of H_3^+ (Upper) and CO (Lower) observed by the Subaru Telescope toward GCS 3-2, the brightest infrared source near the Galactic center. The $R(3, 3)^u$ line (in red) shows the presence of a vast amount of metastable H_3^+ , which signifies high temperature. (Reproduced from ref. 46.)

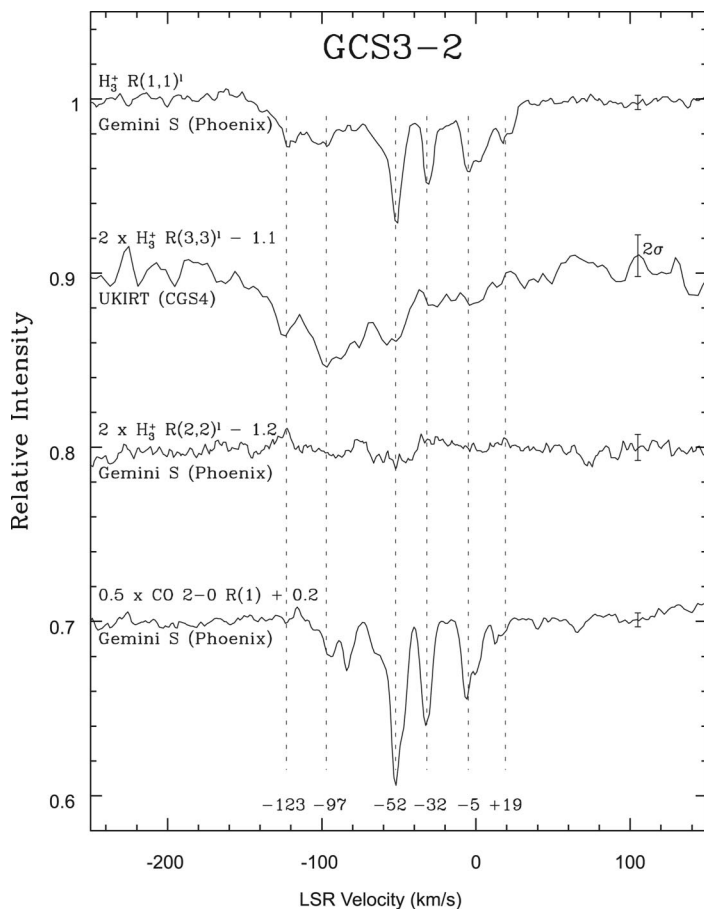


Fig. 6. Observed H_3^+ (top three traces) $R(1, 1)^l$, $R(3, 3)^l$, and $R(2, 2)^l$ lines and CO 2-0 overtone $R(1)$ line toward GCS 3-2 observed by the Gemini South Telescope and the UKIRT. The vertical scaling of the $R(3, 3)^l$ and $R(2, 2)^l$ spectra is multiplied by a factor of 2 and that of the CO spectrum is divided by 2 for clarity. (Reproduced from ref. 57.)

contains many dense molecular clouds with a high volume-filling factor (45, 49). This area, which is perhaps $<10^{-5}$ of the Galaxy in volume, contains a few percent of the total interstellar medium in the Galaxy. Radio-emission lines with critical densities higher than 10^4 cm^{-3} , such as CO $J = 2 \rightarrow 1$, $3 \rightarrow 2$, CS $1 \rightarrow 0$, HCN $1 \rightarrow 0$, etc., provide definitive evidence of high density, whereas emission lines with critical densities lower than 10^3 cm^{-3} such as CO $1 \rightarrow 0$, NH_3 inversion lines (all J, K), and H_2 rotational lines and absorption lines such as OH, H_2CO , etc. do not. Nevertheless high densities had often been claimed from the latter spectra based on circumstantial evidences, and perhaps this contributed to the overestimates of both the volume-filling factor and the fraction of interstellar medium in the CMZ by an order of magnitude (45, 49).

It had also been claimed that a significant portion of the dense clouds had high temperature of 150–300 K from radio and far-infrared spectroscopy. The most direct evidence for this has been the CO emission from high rotational levels such

as $J = 7 \rightarrow 6$ (50, 51) and $J = 16 \rightarrow 15$ (52), but they are limited to the two special regions of high activity, Sgr A and Sgr B (51). A more extensive presence of hot clouds had been claimed using NH_3 in high metastable levels up to (7, 7) (53, 54) and H_2 up to $J = 7$ (55), but the reported densities of 10^4 and $10^{3.5}$ to 10^4 cm^{-3} (56) may well be overestimates.

Our recent observation and analysis of H_3^+ have revealed a vast amount of gas with high temperature ($\approx 250 \text{ K}$) and low density ($n \sim 100 \text{ cm}^{-3}$) in the CMZ (57). The gas has a huge volume and must fill the space between the aforementioned dense clouds. Observed spectra of H_3^+ and CO that provide evidence for this conclusion are shown in Fig. 6.

First, note the similarity between the sharp absorption lines of the $R(1, 1)^l$ spectrum (top trace) and the CO spectrum (bottom trace) with three main peaks at -52 , -32 , and -5 km s^{-1} . They are due to molecules in the cold and relatively dense environment mostly in the intervening spiral arms, the 3-kpc arm, the 4.5-kpc arm (Scutum), and the local arm (Sagittarius), respectively.

Second, note that the CO spectrum is composed largely only of sharp lines, whereas the $R(1, 1)^l$ spectrum shows a deep and wide trough from -150 to $+30 \text{ km s}^{-1}$. We interpret the latter to be due to H_3^+ in the CMZ. The broad relatively featureless absorption reflects the high-velocity dispersion of the gas.

Third, note that the $R(3, 3)^l$ spectrum (second from top) of the metastable H_3^+ is broad and mimics the trough of the $R(1, 1)^l$ spectrum. The strength of the $R(3, 3)^l$ line is definitive evidence for the high temperature of the gas in the CMZ.

Fourth, note that the $R(2, 2)^l$ spectrum (third from top) shows no clear absorption, indicating that the (2, 2) unstable level is not much populated although it is much lower than the (3, 3) level. This strongly inverted population between (2, 2) and (3, 3) due to the $(2, 2) \rightarrow (1, 1)$ spontaneous emission is definitive evidence of the low density of the clouds.

More detailed analyses give more quantitative information on the gas in the CMZ, for which readers are referred to ref. 57. Here, we summarize some main conclusions. Of the total H_3^+ column density of $(4.3 \pm 0.3) \times 10^{15} \text{ cm}^{-2}$ toward GCS 3-2, approximately one-quarter ($1.2 \times 10^{15} \text{ cm}^{-2}$) is in cold clouds mostly in the intervening spiral arms, and the rest is in hot clouds in the CMZ. Approximately half of the latter ($1.6 \times 10^{15} \text{ cm}^{-2}$) is in clouds with velocities near -100 km s^{-1} ; their average temperature is $(270 \pm 70) \text{ K}$, and the density is lower than 50 cm^{-3} , although uncertainty of the latter may be high because of uncertainty of the collision cross section (a factor of 2). The large negative velocity suggests strongly that these clouds are associated with the large-scale structure moving away from the Galactic center at high speed initially proposed as the Expanding Molecular Ring (EMR) (58, 59). It exists at $\approx 180 \text{ pc}$ from the center, at about the border of the CMZ. The remaining H_3^+ with lower velocities are associated with somewhat lower-temperature and higher-density clouds but are all in the CMZ.

The (3, 3) metastable H_3^+ has been detected also toward many other young stars within $\approx 30 \text{ pc}$ of the center. The location of the eight stars so far observed that all showed the metastable spectra are given in Fig. 7. Their spectra show that the hot and diffuse gas is distributed widely in the CMZ, although its velocity depends on the individual sightlines. Readers are referred to ref. 57 for more details of this and many other interesting observations.

Our attempt at detecting metastable H_3^+ in sources in the Galactic disk where high column densities of H_3^+ had been observed has so far been unsuccessful. The warm and diffuse environment seems unique to the CMZ.

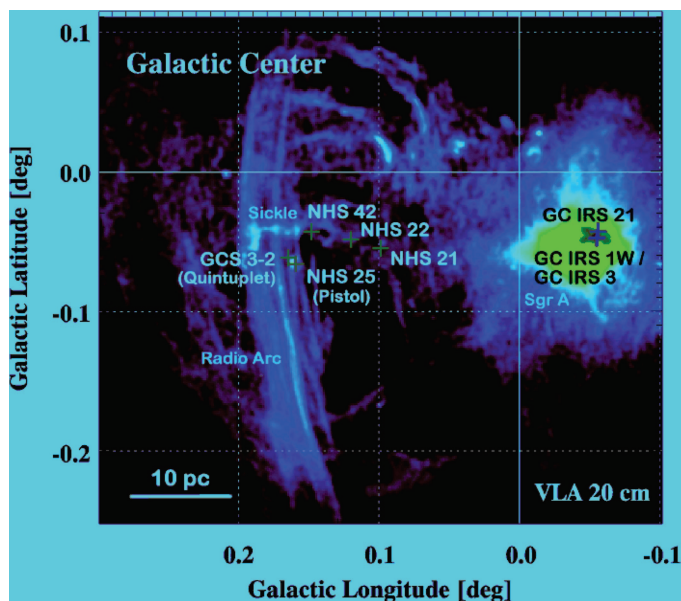


Fig. 7. Location of observed infrared stars indicated by crosses. They all showed the $R(3, 3)'$ spectrum, signifying high temperature, and extremely weak, if any, $R(2, 2)'$ spectrum, signifying low density, indicating the widespread presence of hot and diffuse gas. The background is the VLA 20-cm image by Yusef-Zadeh and Morris (60). (Reproduced from ref. 57.)

Outlook

Our study of the Galactic center using H_3^+ as a probe is in its infancy. The data so far accumulated and the understanding that we are beginning to acquire is but a tip of the iceberg. Many more observations are needed to obtain a comprehensive picture of the hot and diffuse gas in the CMZ. We are in the process of extending the observation from ≈ 30 pc from the center to ≈ 200 pc using other young stars and even some late-type stars distributed over the CMZ. It will take at least a few more years for these observations. Such H_3^+ spectra combined with CO spectra that provide complementary information will help lead us to a better understanding of the gas in the CMZ. Previous to our discovery of the warm and diffuse gas, three categories of gas were known in the CMZ: the dense and mostly cold gas ($T \sim 50$ K) observed by radio-spectra of

OH, NH_3 , CO, CS, HCN etc.; the hot gas with high electron densities observed by radio-wave scattering and free-free emission and absorption measurements; and the ultra-hot gas ($T \sim 10^8$ K) evidenced by the widely observed x-ray emission (45). Observers of each category of the gas claim a high volume-filling factor and yet clearly they cannot coexist in the same region. It will be extremely interesting to find out the relation of the new category of gas to those other gases (60).

The strong signal toward the Galactic center suggests that external galaxies must also have detectable H_3^+ in the center. Indeed, we have detected H_3^+ toward a highly obscured ultraluminous galaxy IRAS 08572 + 3915 NW (61). Because of the expansion of the Universe, the spectrum is red shifted by $z = \Delta\lambda/\lambda = 0.05821$. We plan to observe other ultraluminous galaxies that have strong $3.4\text{-}\mu\text{m}$

aliphatic hydrocarbon absorption, the tell-tale sign of diffuse clouds and hence H_3^+ . Our next plan is to observe the highly obscured active galactic nucleus, the Southern Hemisphere object Superantennae, IRAS 19254-7245. Information obtained from the H_3^+ and CO spectra may provide a new perspective on the nature of active galactic nuclei.

Because cosmic-ray ionization is ubiquitous, H_3^+ is produced abundantly in any region with molecular hydrogen, although its steady-state concentration is not high due to its high chemical reactivity. As long as the pathlength in a cloud is sufficiently large, H_3^+ will be detectable in any object. We have a considerable amount of data yet to be published on dense and diffuse clouds. In 2002, H_3^+ emission from the young star HD 141569A was reported as possibly from preplanetary gas orbiting the star (62). Unfortunately, our attempt to confirm this emission ended up negating the original claim (63). However, detecting H_3^+ in protoplanets and extra-solar planets remains an intriguing possibility. Our proposal to search for H_3^+ in planetary nebulae and protoplanetary nebulae was accepted this year by the Subaru Telescope after several attempts.

Clearly there is no shortage of interesting objects to observe. The simplicity of the H_3^+ chemistry allows us to obtain fresh and unique astrophysical information from observed spectra. We are thrilled by the prospect of obtaining unexpected new information. The next 10 years will be full of surprises.

Works discussed in this paper result from collaboration with T. R. Geballe, with whom I have been working on the project of interstellar H_3^+ since 1982. We were later joined by B. J. McCall in 1996 and M. Goto and T. Usuda in 2000. To all of them I am deeply indebted. I am grateful to T. R. Geballe, B. J. McCall, and C. Chung for their critical reading of the manuscript. My work has been supported by a succession of National Science Foundation grants, most recently Grant PHY 03-54200.

- Thomson, J. J. (1911) *Philos. Mag.* **21**, 225–249.
- Hogness, T. R. & Lunn, E. G. (1925) *Phys. Rev.* **26**, 44–55.
- Martin, D. W., McDaniel, E. W. & Meeks, M. L. (1961) *Astrophys. J.* **134**, 1012–1013.
- Watson, W. D. (1973) *Astrophys. J.* **183**, L17–L20.
- Herbst, E. & Klempner, W. (1973) *Astrophys. J.* **185**, 505–533.
- Thronson, H. A. & Shull, J. M., eds. (1990) *The Interstellar Medium in Galaxies* (Kluwer, Dordrecht, The Netherlands).
- Anicich, V. G. & Huntress, W. T., Jr. (1986) *Astrophys. J. Suppl.* **62**, 553–672.
- Sofia, U. J., Lauroesch, J. T., Meyer, D. M. & Cartledge, S. I. B. (2004) *Astrophys. J.* **605**, 272–277.
- McCall, B. J., Huneycutt, A. J., Saykally, R. J., Djuric, N., Dunn, G. H., Semaniak, J., Novotny, O., Al-Khalili, A., Ehlerding, A., Helbey, F., et al. (2004) *Phys. Rev. A* **70**, 052716.
- Coulson, C. A. (1935) *Proc. Cambridge Philos. Soc.* **31**, 244–259.
- Oka, T. (1983) in *Molecular Ions: Spectroscopy, Structure, and Chemistry*, eds. Miller, T. A. & Bondybey, V. E. (North-Holland, Amsterdam), pp. 73–90.
- Carney, G. D. & Porter, R. N. (1976) *J. Chem. Phys.* **65**, 3547–3565.
- Pine, A. S. (1974) *J. Opt. Soc. Am.* **64**, 1688–1690.
- Oka, T. (1980) *Phys. Rev. Lett.* **45**, 531–534.
- Oka, T. (1981) *Philos. Trans. R. Soc. London A* **303**, 543–549.
- Oka, T. (1992) *Rev. Mod. Phys.* **64**, 1141–1149.
- Miller, S., Achilleous, N., Ballestes, G. E., Geballe, T. R., Joseph, R. D., Prangé, R., Rego, D., Stallard, T., Tennyson, J., Traflet, L. M., et al. (2000) *Philos. Trans. R. Soc. London A* **358**, 2485–2502.
- Geballe, T. R. & Oka, T. (1996) *Nature* **384**, 334–335.
- van Dishoeck, E. F. & Black, J. H. (1986) *Astrophys. J. Suppl.* **62**, 109–145.
- Lee, H.-H., Bettens, R. P. A. & Herbst, E. (1996) *Astron. Astrophys. Suppl.* **119**, 111–114.
- Miller, S. (November 28, 1996) *The Guardian*.
- Barthélémy, P. (November 30, 1996) *Le Monde*, Section Aujourd'hui Sciences, p. 25.
- McCall, B. J., Geballe, T. R., Hinkle, K. H. & Oka, T. (1999) *Astrophys. J.* **522**, 338–348.
- Roberts, H., Herbst, E. & Millar, T. J. (2003) *Astrophys. J.* **591**, L41–L44.

25. Roberts, H., Herbst, E. & Millar, T. J. (2004) *Astron. Astrophys.* **424**, 905–917.
26. Geballe, T. R., McCall, B. J., Hinkle, K. H. & Oka, T. (1999) *Astrophys. J.* **510**, 251–257.
27. Massey, P. & Thompson, A. B. (1991) *Astrophys. J.* **101**, 1408–1428.
28. McCall, B. J., Geballe, T. R., Hinkle, K. H. & Oka, T. (1998) *Science* **279**, 1910–1913.
29. Bohlin, R. C., Savage, B. D. & Drake, J. F. (1978) *Astrophys. J.* **224**, 132–142.
30. Larsson, M. (2000) *Philos. Trans. R. Soc. London A* **358**, 2359–2559.
31. Kokoouline, V. & Greene, C. H. (2003) *Phys. Rev. Lett.* **90**, 133201.
32. Cravens, T. E. & Dalgarno, A. (1978) *Astrophys. J.* **219**, 750–752.
33. Harquist, T. W., Black, J. H. & Dalgarno, A. (1978) *Mon. Not. R. Astron. Soc.* **185**, 643–646.
34. Harquist, T. W., Doyle, H. T. & Dalgarno, A. (1978) *Astron. Astrophys.* **68**, 65–67.
35. Liszt, H. S. (2003) *Astron. Astrophys.* **398**, 621–630.
36. McCall, B. J., Hinkle, K. H., Geballe, T. R., Moriarty-Schieven, G. H., Evans, N. J., II, Kawaguchi, K., Takano, S., Smith, V. V. & Oka, T. (2002) *Astrophys. J.* **567**, 391–406.
37. Oka, T. & Jagod, M.-F. (1993) *J. Chem. Soc. Faraday Trans.* **89**, 2147–2154.
38. Oka, T., Shimizu, F. O., Shimizu, T. & Watson, J. K. G. (1972) *Astrophys. J.* **165**, L15–L19.
39. Pan, F.-S. & Oka, T. (1986) *Astrophys. J.* **305**, 518–525.
40. Neale, L., Miller, S. & Tennyson, J. (1996) *Astrophys. J.* **464**, 516–520.
41. Oka, T. & Epp, E. (2004) *Astrophys. J.* **613**, 349–354.
42. van Vleck, J. H. & Weiskopf, V. F. (1945) *Rev. Mod. Phys.* **17**, 227–236.
43. Oka, T. (1973) *Adv. At. Mol. Phys.* **9**, 127–206.
44. Cordonnier, M., Uy, D., Dickson, R. M., Kerr, K. E., Zhang, Y. & Oka, T. (2000) *J. Chem. Phys.* **113**, 3181–3193.
45. Morris, M. & Serabyn, E. (1996) *Annu. Rev. Astron. Astrophys.* **34**, 645–701.
46. Geballe, T. R. (2000) *Philos. Trans. R. Soc. London A* **358**, 2503–2513.
47. Goto, M., McCall, B. J., Geballe, T. R., Usuda, T., Kobayashi, N., Terada, H. & Oka, T. (2002) *Publ. Astron. Soc. Japan* **54**, 951–961.
48. Figer, D. F., McLean, I. S. & Morris, M. (1999) *Astrophys. J.* **514**, 202–220.
49. Mezger, P. G., Duschl, W. J. & Zylka, R. (1996) *Astron. Astrophys. Rev.* **7**, 289–388.
50. Harris, A. I., Jaffe, D. T., Silber, M. & Genzel, R. (1985) *Astrophys. J.* **294**, L93–L97.
51. Kim, S., Martin, C. L., Stark, A. A. & Lane, A. P. (2002) *Astrophys. J.* **580**, 896–903.
52. Genzel, R., Watson, D. M., Crawford, M. K. & Townes, C. H. (1985) *Astrophys. J.* **297**, 766–786.
53. Mauersberger, R., Henkel, C., Wilson, T. L. & Walmsley, C. M. (1986) *Astron. Astrophys.* **162**, 199–210.
54. Hüttemeister, S., Wilson, T. L., Bania, T. M. & Martín-Pintado, J. (1993) *Astron. Astrophys.* **280**, 255–267.
55. Rodríguez-Fernandes, N. J., Martín-Pintado, J., Fuente, A., de Vicente, P., Wilson, T. L. & Hüttemeister, S. (2001) *Astron. Astrophys.* **365**, 174–185.
56. Hüttemeister, S., Dahmen, G., Mauersberger, R., Henkel, C., Wilson, T. L. & Martín-Pintado, J. (1998) *Astron. Astrophys.* **334**, 646–658.
57. Oka, T., Geballe, T. R., Goto, M., Usuda, T. & McCall, B. J. (2005) *Astrophys. J.* **632**, 882–893.
58. Kaifu, N., Kato, T. & Iguchi, T. (1972) *Nature* **283**, 105–107.
59. Scoville, N. Z. (1972) *Astrophys. J.* **175**, L127–L132.
60. Boldyrev, S. & Yusef-Zadeh, F. (2006) *Astrophys. J.* **637**, L101–L104.
61. Geballe, T. R., Goto, M., Usuda, T., Oka, T. & McCall, B. J. (2006) *Astrophys. J.*, in press.
62. Brittain, S. D. & Rettig, T. W. (2002) *Nature* **418**, 57–59.
63. Goto, M., Geballe, T. R., McCall, B. J., Usuda, T., Suto, H., Terada, H., Kobayashi, N. & Oka, T. (2005) *Astrophys. J.* **629**, 865–872.
64. Kokoouline, V. & Greene, C. H. (2003) *Phys. Rev. A* **68**, 012703.